A PHOENIX MODEL ATMOSPHERE GRID FOR GAIA

I. Brott[1,2], **P.H. Hauschildt**[1]

[1]Hamburger Sternwarte, Gojenbergsweg 112, 21029 Hamburg, Germany
[2]INTEGRAL Science Data Centre, Chemin d'Ecogia 16, 1290 Versoix, Switzerland

ABSTRACT

We present the results of a set of model atmospheres and synthetic spectra computed with the PHOENIX code. The models cover a range of effective temperatures (2 700 K $\leq T_{\rm eff} \leq$ 10 000 K), gravities ($-0.5 \leq \log(g) \leq 5.5$) and metallicities ($-4.0 \leq [Z/H] \leq +0.5$). In addition, variations of alpha elements are considered for each metallicity. The models are computed with a homogeneous set of input data in order to allow for direct relative comparison between the models. For example, all models use a mixing length of l/H_p = 2.0. We provide synthetic spectra with a resolution of 0.2 nm from the UV to the infrared for all models. We give a brief overview of the input physics and show illustrative results. All synthetic spectra are available via ftp.

Key words: Stars: atmospheres; Stars: late-type; Radiative transfer; Gaia.

1. INTRODUCTION

Model atmospheres and synthetic spectra are of fundamental importance in the development of filter and resolution systems and also helpful for the design of the analysis packages for the Gaia mission. Here, we present our first results of a grid of model atmospheres and synthetic spectra computed with the PHOENIX v13 code (Hauschildt & Baron 1999). The grid covers the parameter range of interest for the Gaia community (see Table 1), $\sim$ 44 000 models and spectra in total. It is publicly available via ftp[1].

1.1. The PHOENIX Code

PHOENIX is a multi-purpose stellar atmosphere code used to compute A-T dwarfs, giants, O-B stars and stellar winds, exoplanet atmospheres (also irradiated), nova atmospheres, SNe I & II and CVs. It was developed by our group to be a very general NLTE stellar atmosphere code (Hauschildt 1992, 1993, 1995; Allard & Hauschildt 1995; Baron et al. 1996; Hauschildt et al. 1996, 1997; Baron & Hauschildt 1998; Allard et al. 2001; Hauschildt et al. 2001) . The code can handle extremely large model atoms as well as line blanketing by many millions of atomic and molecular lines. The radiative transfer in PHOENIX is solved in spherical geometry and includes the effects of special relativity (including advection and aberration) in the models. The PHOENIX code also allows us to include a large number of NLTE and LTE background lines and to solve the radiative transfer equation for each of them *without* using simplifying approximations. Therefore, the line profiles must be resolved in the co-moving (Lagrangian) frame, which requires many wavelength points (typically 50 000 in the Gaia grid). Details of the numerical methods used in PHOENIX can be found in the literature cited above. In order to take advantage of the enormous computing power and vast memory sizes of modern parallel computers, we have developed a parallel version of PHOENIX which is now the default production version for all our model grids.

[1]ftp.hs.uni-hamburg.de/pub/outgoing/phoenix/GAIA

Table 1. Grid Parameters.

Parameter	Range	Step
$T_{\rm eff}$	2700 . . . 5000 K	100 K
	5000 . . . 10 000 K	200 K
log g	-0.5 . . . 5.5	0.5
$[Z/H]$	$+0.5$ . . . -3.5	0.5
$[\alpha/\alpha_\odot]$	-0.2 . . . $+0.8$	0.2

2. MODEL ASSUMPTIONS

The models of the Gaia grid are calculated for **1D spherical symmetry** and a fixed stellar mass of 1 $M_\odot$ for simplicity. Our basic assumptions for the grid presented here are time independence, hydrostatic and thermal equilibrium, and LTE. Convection is treated with a mixing length of l/H_p = 2.0.

The micro-physics setup is similar to the one used in our latest model grids (Allard et al. 2001), which give the currently best fits to the observed spectra of M, L, and T dwarfs. Water- and TiO-lines are taken from the

AMES calculation from Partridge & Schwenke (1997) and Schwenke (1998). Our combined molecular line lists include about 700 million molecular lines. Typically about 15–300 million of these are selected in a model. Atomic and molecular line opacities are selected dynamically for the relevant LTE background lines from the master line lists and sum the contribution of every line within a search window to compute the total line opacity at *arbitrary* wavelength points. We do not use pre-computed opacity tables but individual line profiles. This approach allows detailed and depth dependent line profiles to be used during the iterations. This is important e.g., for M dwarf spectra where line broadening and blanketing are crucial for the model structure and therefore the computation of the synthetic spectra. For details see Hauschildt et al. (2003).

In the present models we have included a constant statistical velocity field, $\chi = 2$ km s^{-1}, which is treated like a microturbulence. Lines are chosen if they are stronger than a threshold, $\Gamma \equiv \xi_l/\kappa_c = 10^{-4}$, where ξ_l and κ_c are the extinction coefficient of the line at its centre and the local $b-$f absorption coefficient, respectively. Details of the line selection process are given in Hauschildt et al. (1999a,b).

The equation of state (EOS) is an enlarged and enhanced version of the EOS used in Allard & Hauschildt (1995). About 1000 species (atoms, ions, molecules) are included. For cooler models, the formation of dust particles has to be considered in the EOS. In our cooler models we have used the assumption that dust forms and immediately rains out completely below the photosphere. For effective temperatures above 2700 K, dust formation can be neglected and therefore this assumption is not critical for the Gaia grid.

3. THE GAIA GRID

In the following, we will show some examples from the Gaia grid. Varying one model parameter while keeping the others fixed, we generated a series of plots to demonstrate the behavior of the stellar spectrum. A review about the quality of the synthetic spectra is given in Kučinskas et al. (2005).

Figure 1 shows the effect of temperature variation on a model atmosphere. At lower temperatures metals become important opacity sources especially in the UV, shifting the flux maximum of the spectrum to longer wavelengths. At higher temperatures metals are ionized and the spectrum is dominated by hydrogen. This effect is independent from the metallicity (upper and lower part of Figure 1).

Increasing the metallicity as shown in Figure 2, resulting metal lines dominate the spectrum especially in the UV region.

By varying the gravity, we observe different effects (Figure 3): Hot, metal-poor models show a more pronounced Balmer jump with lower gravities (top panel), whereas in metal-rich models (middle and lower panel) the gravity

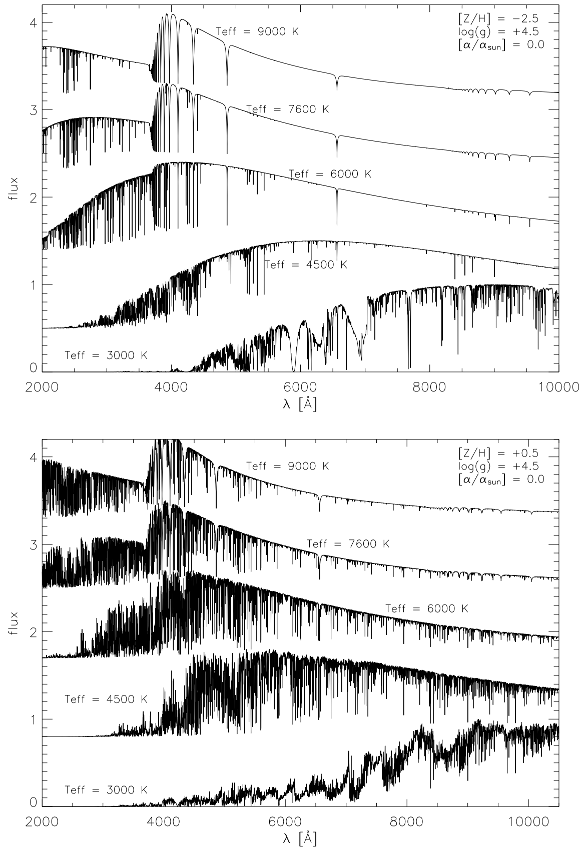

Figure 1. The effect of temperature variation on a model with different metallicities and parameters as indicated in the figure. At lower temperatures (< 4000 K) metals become important opacity sources especially in the UV, shifting the flux maximum of the spectrum to longer wavelengths, while at higher temperatures (> 7000 K metals are ionized such that hydrogen is dominating the spectrum.

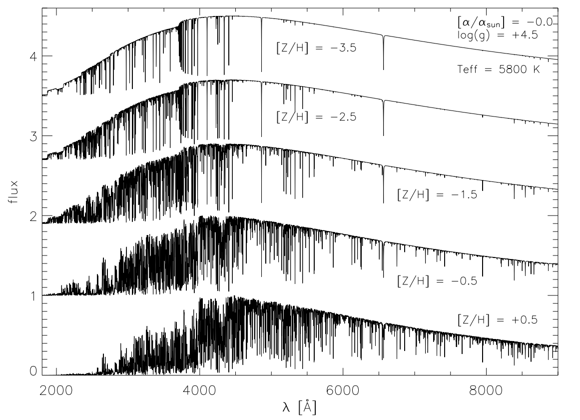

Figure 2. Models with $T_{\rm eff}$ =5800 K and different metallicity. With increasing metallicity more and more metal lines appear. Especially in the UV the spectrum is dominated by metal opacity.

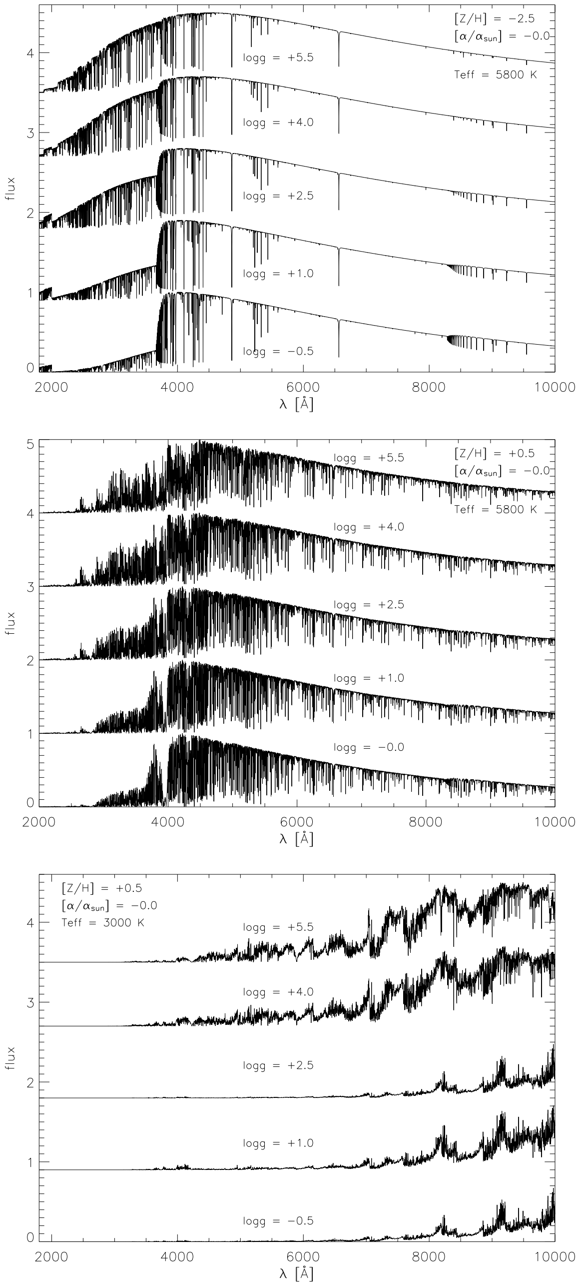

Figure 3. By varying the gravity, we observe different effects. At high temperatures (top panel) the Balmer jump gets more pronounced with lower gravities. At high metallicities it can have an important effect on molecular lines as shown in the lower panel for a $[Z/H]$ =+0.5, $T_{\rm eff}$ = 3000 K model, because the high pressure influences the EOS, resulting in larger concentration of molecules. The middle panel shows an intermediate state.

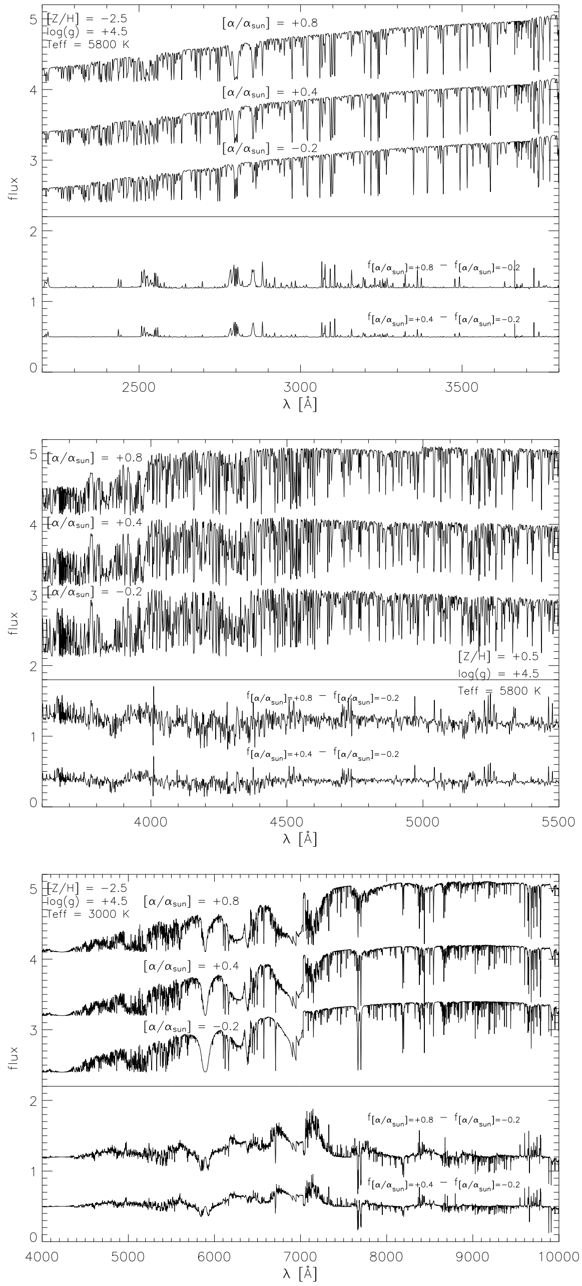

Figure 4. The variation of the spectrum with changing α-element abundance (compared to the solar value). The top panel shows a model with $[Z/H] = -2.5$. To emphasize the effect of α-element abundances we show the difference spectra in the lower part of each panel. The middle panel shows a model with the same parameters as above but a higher metallicity $[Z/H] = +0.5$, and the lower panel a 3000 K model. This shows that α-elements become more important in cool and/or metal rich atmospheres. Note that cool models are influenced over larger wavelengths ranges.

can have important effects on the formation of molecular lines. The high pressure influences the EOS, resulting in a larger concentration of molecules.

The Gaia grid also includes different α-element abundances for each set of parameters. Some are shown in Figure 4. We have varied the abundance of the α-elements O, Ne, Mg, Si, S, Ca, Ti in our models. The effect of α-element abundances is small, so each panel shows also the difference spectra as well. Comparing the middle and lower panel of Figure 4 one sees, that α-element abundances become important at low temperatures and/or high metallicities.

4. CONCLUSIONS & OUTLOOK

The present Gaia grid provides a very detailed set of synthetic spectra to support the photometric working groups. We plan a full extension of the grid to the temperature range between 10 000 K and 50 000 K. These calculations will be done in full NLTE. It is also possible to extend the present synthetic spectra to higher resolution upon request to the authors.

ACKNOWLEDGMENTS

PHH was supported in part by the Pôle Scientifique de Modélisation Numérique at ENS-Lyon. Some of the calculations presented here were performed at the Höchstleistungs Rechenzentrum Nord (HLRN), at the National Energy Research Supercomputer Center (NERSC), supported by the U.S. DOE, and at the San Diego Supercomputer Center (SDSC), supported by the NSF. We thank all these institutions for a generous allocation of computer time.

REFERENCES

Allard, F., Hauschildt, P. H. 1995, ApJ, 445, 433

Allard, F., Hauschildt, P. H., Alexander, D. R., Tamanai, A., Schweitzer, A. 2001, ApJ, 556, 357

Baron, E., Hauschildt, P. H. 1998, ApJ, 495, 370

Baron, E., Hauschildt, P. H., Nugent, P., Branch, D. 1996, MNRAS, 283, 297

Hauschildt, P. H. 1992, JQSRT, 47, 433

Hauschildt, P. H. 1993, JQSRT, 50, 301

Hauschildt, P. H. 1995, JQSRT, 54, 987

Hauschildt, P. H., Allard, F., Baron, E. 1999a, ApJ, 512, 377

Hauschildt, P. H., Allard, F., Baron, E., Aufdenberg, J., Schweitzer, A. 2003, in ASP Conf. Ser. 298: GAIA Spectroscopy: Science and Technology, 179

Hauschildt, P. H., Allard, F., Ferguson, J., Baron, E., Alexander, D. R. 1999b, ApJ, 525, 871

Hauschildt, P. H., Baron, E. 1999, J. of Comp. and Appl. Math., 102, 41

Hauschildt, P. H., Baron, E., Allard, F. 1997, ApJ, 483, 390

Hauschildt, P. H., Baron, E., Starrfield, S., Allard, F. 1996, ApJ, 462, 386

Hauschildt, P. H., Lowenthal, D. K., Baron, E. 2001, ApJS, 134, 323

Kučinskas, A., Brott, I., Hauschildt, P. H., et al. 2005, ESA SP-576, this volume

Partridge, H., Schwenke, D. W. 1997, J. Chem. Phys., 106, 4618

Schwenke, D. W. 1998, in Chemistry and Physics of Molecules and Grains in Space. Faraday Discussions No. 109, 321